Journal of Geophysical Research: Atmospheres

RESEARCH ARTICLE
10.1029/2018JD029121

Solar Effects on the Atmospheric Electric Field During 2010–2015 at Low Latitudes

J. Tacza[1], J.-P. Raulin[1], R. R. S. Mendonca[2,3], V. S. Makhmutov[4], A. Marun[5], and G. Fernandez[6]

[1]Center of Radio Astronomy and Astrophysics Mackenzie, Engineering School, Mackenzie Presbyterian University, São Paulo, Brazil, [2]State Key Laboratory of Space Weather, National Space Science Center, Chinese Academy of Sciences, Beijing, China, [3]National Institute for Space Research, Sao Jose dos Campos, Brazil, [4]Lebedev Physical Institute, Russian Academy of Sciences, Moscow, Russia, [5]Instituto de Ciencias Astronómicas de la Tierra y el Espacio, San Juan, Argentina, [6]Complejo Astronómico El Leoncito, San Juan, Argentina

Key Points:
- Solar flare photons are unlikely to affect the global atmospheric electric circuit at low latitudes
- Solar proton events enhance the conductivity above thunderstorms resulting in an atmospheric electric field increase in fair weather regions at low latitudes
- Ground level enhancement that occurred on 17 May 2012 was capable to produce an atmospheric electric field decrease in fair weather conditions at low-latitude regions

Correspondence to:
J. Tacza,
josect1986@gmail.com

Citation:
Tacza, J., Raulin, J.-P., Mendonca, R. R. S., Makhmutov, V. S., Marun, A., & Fernandez, G. (2018). Solar effects on the atmospheric electric field during 2010–2015 at low latitudes. *Journal of Geophysical Research: Atmospheres, 123*, 11,970–11,979. https://doi.org/10.1029/2018JD029121

Received 4 JUN 2018
Accepted 18 OCT 2018
Accepted article online 23 OCT 2018
Published online 9 NOV 2018

Abstract Solar phenomena such as flares and solar energetic particles events are potential candidates to affect the global atmospheric electric circuit. One can study these effects using measurements of the atmospheric electric field in fair weather regions. In this paper, we investigate deviations of the atmospheric electric field daily curve during solar disturbances (solar flares and solar proton events) from mean values obtained in fair weather conditions. Using the superposed epoch analysis, in order to enhance the visualization of small effects, we study the atmospheric electric field data observed between January 2010 and December 2015 at the Complejo Astronómico El Leoncito, San Juan, Argentina. The results show no deviation of the atmospheric electric field after solar flares, and an increase of about 10 V/m after solar proton events. The last result suggests possible ionization effects above thunderstorm in disturbed weather regions, which alters the global atmospheric electric circuit. On the other hand, we analyze the variation of the atmospheric electric field during a ground level enhancement on 17 May 2012, which was capable to produce changes on the surface electric field.

1. Introduction

The atmospheric electric field (AEF) persists in regions of fair weather (FW) and shows a typical daily variation, hereafter called a FW standard curve. Fair weather regions are those areas with no local electrification processes, and without appreciable convective cloud extent, that is, no low stratus cloud and less than three-eighth cumuliform cloud (Harrison, 2013). This FW standard curve is thought to be mostly maintained by thunderstorms activity in remote regions, also called disturbed weather regions (Whipple, 1929). The relationship between the atmospheric electric field and thunderstorm activity supports the idea of a global atmospheric electric circuit (GAEC) initially suggested by Wilson (1921).

The global atmospheric electric circuit is formed between the Earth's surface and the lower atmosphere (Haldoupis et al., 2017), linking charge separation in disturbed weather regions with current flows in fair weather regions. In disturbed weather regions, there are "electric batteries," such as thunderstorms, causing ascending vertical currents (i.e., from thundercloud top to the atmosphere). On the other hand, in fair weather regions, there are descending vertical currents (i.e., from the atmosphere to the ground). Finally, the electric circuit is closed by currents that flow from (i) fair weather to disturbed weather regions through the rocks and the oceans of the Earth's surface and (ii) from disturbed weather to fair weather regions through the upper circuit boundary (Rycroft et al., 2008). The global atmospheric electric circuit is mainly driven by thunderstorms and electrified rain/shower clouds (Liu et al., 2010; Wilson, 1921). Moreover, mean contributions to the GAEC from land and ocean thunderstorm are 1.1 and 0.7 kA, respectively. Contributions of electrified shower clouds are 0.22 kA for ocean and 0.04 kA from land (Mach et al., 2011). Additionally, energetic charged particles from space can also drive the GAEC, that is, solar energetic particles, especially, at high latitudes (Rycroft et al., 2012; Sapkota & Varshneya, 1990).

Solar energetic particles (SEPs) constitute a population of energetic charged particles ejected by the Sun during transient events, which can be sporadically observed as a rapid enhancement of charged particle flux in the space near to the Earth. An event may last from hours to days depending on the particle energy and with a decay that is usually much longer than its growth. The bulk of solar energetic particles are protons; thus, the episodes of SEP occurrence are sometimes called "solar proton events (SPEs)" (e.g., Bazilevskaya, 2005). High-

energy protons that hit the Earth during SEP events lose their energy throughout interactions with the air nuclei producing secondary particles. In this way, they initiate nuclear-electromagnetic cascades in the atmosphere. Secondary nucleons, mostly neutrons, can sometimes reach the ground level and thus be observed by neutron monitors. Such events are called ground level enhancements (GLEs; Bazilevskaya, 2005).

Ionization by solar proton events can result in changes of the lower atmosphere conductivity height profile (Kokorowski et al., 2012; Mironova et al., 2015; Velinov et al., 2013, and references therein). Data obtained by balloon-borne sensors at ~30 km revealed an increase of the electrical conductivity and a decrease of the atmospheric electric field in fair weather regions after SPEs (Holzworth et al., 1987; Holzworth & Mozer, 1979; Kokorowski et al., 2006; Reagan et al., 1983). Such opposite and simultaneous response can be understood if one assumes continuity of the air-Earth current density with altitude in fair weather regions. In other words, the product of conductivity (σ) and electric field (E) should be constant with altitude in order to fulfill Ohm's law (Haldoupis et al., 2017). Furthermore, changes in the atmospheric electric field and the atmospheric electric current at ground level have been detected after solar proton events (Elhalel et al., 2014; Nicoll & Harrison, 2014).

Several authors developed models in order to explain how solar proton events can modulate the global atmospheric electric circuit (Farrell & Desch, 2002; Markson, 1978; Willett, 1979). These models proposed that solar proton events result in an increase of the ionization rate above thunderstorms producing an increase of the electrical conductivity. This causes a decrease in the resistance between the top of the thunderstorm and the ionosphere, allowing more current to flow upward and, therefore, through of the global electric circuit. Consequently, we have an increase of the charge accumulation at the top boundary of the global electric circuit generating an enhancement of the electrical potential in fair weather regions and, thus, increasing the atmospheric electric field. This has been evidenced in some works where the increase of the AEF lasted until three to four days after the start of solar flares (Cobb, 1967; Reiter, 1969; Reiter, 1971; Sartor, 1980; Sheftel et al., 1994; Takagi & Iwata, 1984). However, in these works, the period of time analyzed included many solar, interplanetary, and geomagnetic phenomena, such as solar flare photons, solar proton events, coronal mass ejections, Forbush decreases, and intense geomagnetic storms. Therefore, in order to better understand the role of these phenomena on the global electric circuit, it is necessary to isolate and study separately each of them.

In this paper, we study the variations of the atmospheric electric field curve observed in fair weather conditions during two types of solar events: (I) solar flares (observed without solar proton events occurrence) and (II) solar proton events. We use atmospheric electric field data recorded between January 2010 and December 2015 at the Complejo Astronómico El Leoncito (CASLEO; latitude 31.798°S, longitude 69.295°W, altitude 2,552 m above sea level (asl), geomagnetic rigidity cutoff R_c ~9.8 GV). In section 2, the observation site and instrumentation are presented. The data analysis and results are presented in sections 3 and 4, respectively. The final section presents the discussions and summarizes the conclusions of this study.

2. Observation Site and Instrumentation

CASLEO is an astronomical observatory (latitude 31.798°S, longitude 69.295°W, altitude 2,552 m asl) located in "El Leoncito," an area characterized with more than 250 clear-sky days per year, no clouds, almost no wind blowing, and a typically diaphanous, contamination-free atmosphere. Furthermore, the water vapor content is scarce (APRE (IT) & DST (ZA), 2013). El Leoncito is located in the Department of Calingasta in the Province of San Juan, Argentina, 40 km away from the town of Barreal, facing a geological structure called "Barreal Blanco" (APRE (IT) & DST (ZA), 2013). Located far from the city and most of the year with clear sky, makes El Leoncito an optimal place for atmospheric electric field measurements in fair weather conditions. The fair weather conditions are defined by days with wind speed $<$8 m/s, no rain, and low cloud cover at the measurement site. The meteorological data used in this research are provided from a station located 1.5 km from CASLEO. From April 2018, a new meteorological station device is available close to the electric field sensor.

In CASLEO, continuous measurements of the atmospheric electric field are recorded with two electric field mill sensors, called CAS1 and CAS2, and separated by ~0.4 km between each other. The principle of electric field mill operation is based on the fundamental laws of electromagnetism. When a conducting plate is exposed to an electric field, a charge is induced proportional to the electric field and to the plate area. More details about the electric field mill sensor can be found in Secker (1975). These sensors are part of

the Atmospheric electric Field Network in South America (https://theafinsa.wordpress.com). Strictly speaking, the electric field sensor measures the atmospheric electric potential gradient (PG = $-E_z$, where E_z is the vertical atmospheric electric field). In this study, PG measurements will be described as AEF measurements. AEF intensities are measured with a time resolution of 0.5 s, and afterward integrated using 180-min averages for the analysis reported here. Then, AEF intensities are corrected to account for the height of the local sensor mounting, which otherwise would result in overestimated readings (Chubb, 2014). In a previous work, Tacza et al. (2014) have shown that the AEF daily curve at CASLEO has a mean value of about 80 V/m and shows a good correlation with the universal Carnegie curve ($R = 0.9$). This indicates the possibility of providing reliable diurnal variations curve, in fair weather conditions, in order to analyze solar phenomena.

In this study, the main atmospheric electric field data set used is that from CAS2 station, since it represents the longest coverage of about six-year measurements. The methodology applied to analyze these data is explained in the following section.

3. Data Analysis

We analyze the fair weather curve variation of the atmospheric electric field for two different types of solar events: (I) solar flares with an X-ray peak flux greater than GOES-Class C1, and not followed by any solar energetic particle events, and (II) intense solar proton events with significant proton flux above 100 MeV as detected by GOES particle instruments. To get rid of the effects of other solar and/or geomagnetic disturbances, we choose solar flares and solar proton events such that *Kp* index remains lower than 4 during three consecutive days, that is, one day before and two days after the events. Similarly, we disregard events for which a Forbush decrease occurred during this three-day period. Finally, during this three-day period around the solar event, we remove hourly values of atmospheric electric field for which high wind speed or lightning were detected.

The methodology adopted in the analysis is as follows: first, monthly mean curves of the atmospheric electric field diurnal variations in fair weather conditions were calculated for each month (monthly standard curve). Second, for each solar event, a time window of 24 hr before and 48 hr after the start time of the event is used, and the start time of the solar flare is defined as the beginning of the X-ray 1–8 Ang. flux enhancement. Similarly, the start time of SPEs is defined as the beginning of ≥100 MeV proton flux enhancement at the satellite. Third, the difference between the AEF values, of every time window, and their monthly standard curves were calculated to get AEF excesses. Finally, we applied the superposed epoch analysis (SEA) to the excesses curves. The last two steps can be summarized by the following formula:

$$E_{\mathrm{SEA}} = \frac{1}{N}\sum_{i=1}^{N} E_i - \overline{E}_i$$

where E_{SEA} is the atmospheric electric field excess deduced after the superposed epoch analysis, N is the number of events, E_i is the 3-hr average atmospheric electric field for event i, and $\overline{E}_i$ is the 3-hr average value of the FW AEF monthly standard curve corresponding to event i.

In order to compare the results, we applied the same methodology to three-day periods of atmospheric electric field measurements without solar flares or solar proton events. In this case, the time zero for applying the superposed epoch analysis was chosen at different time during the day to not restrict the result for a specific time. This ends with a "background" curve characteristics of the atmospheric electric field variations without any solar disturbances.

4. Results

This work characterizes the behavior of the atmospheric electric field, in relation to solar events, measured by ground-based sensors installed at low-latitude regions. The following subsections show the results found.

4.1. Atmospheric Electric Field Response to Solar Flare Events

Figure 1 shows the result of case I obtained using the method described above applied to 114 solar flares events (black curve). The background level (red curve) is obtained on the same manner from 46 fair weather days without solar flares. The error bar represents two standard errors of the mean. This figure shows that the

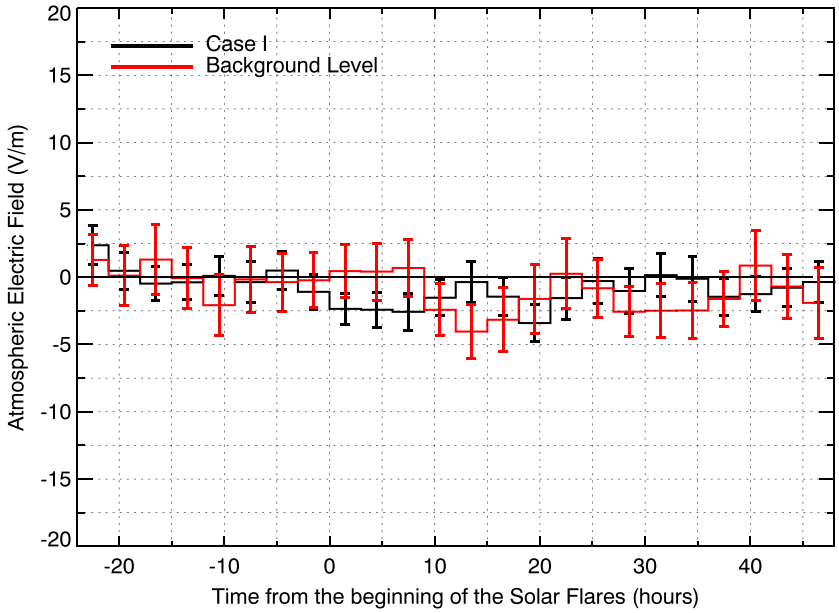

Figure 1. Superposed epoch analysis of the atmospheric electric field deviation response to solar flare events (black curve) and to random selected fair weather periods (red curve). The time zero is the start time of the solar flare. The error bars represent two standard errors of the mean.

variability in both curves are between ±4 V/m, evidencing that no significant effects on the atmospheric electric field values are found during 48 hr since the start of the solar flare.

4.2. Atmospheric Electric Field Response to Solar Proton Events

Figure 2 shows the result of case II obtained from the composite of 15 solar proton events (black curve). The error bar represents two standard errors of the mean. Similarly as in Figure 1, Figure 2 shows the background level (red curve) with its respective error bar. A clear increase of ~10 V/m on the atmospheric electric field

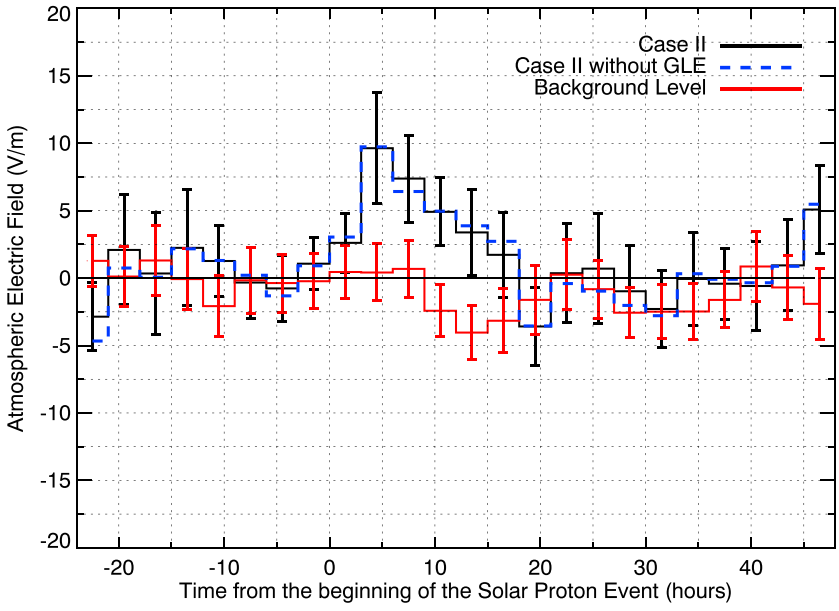

Figure 2. As described in Figure 1 but for the solar proton events (case II). The blue dashed curve shows the results of the superposed epoch analysis without the event of 17 May 2012.

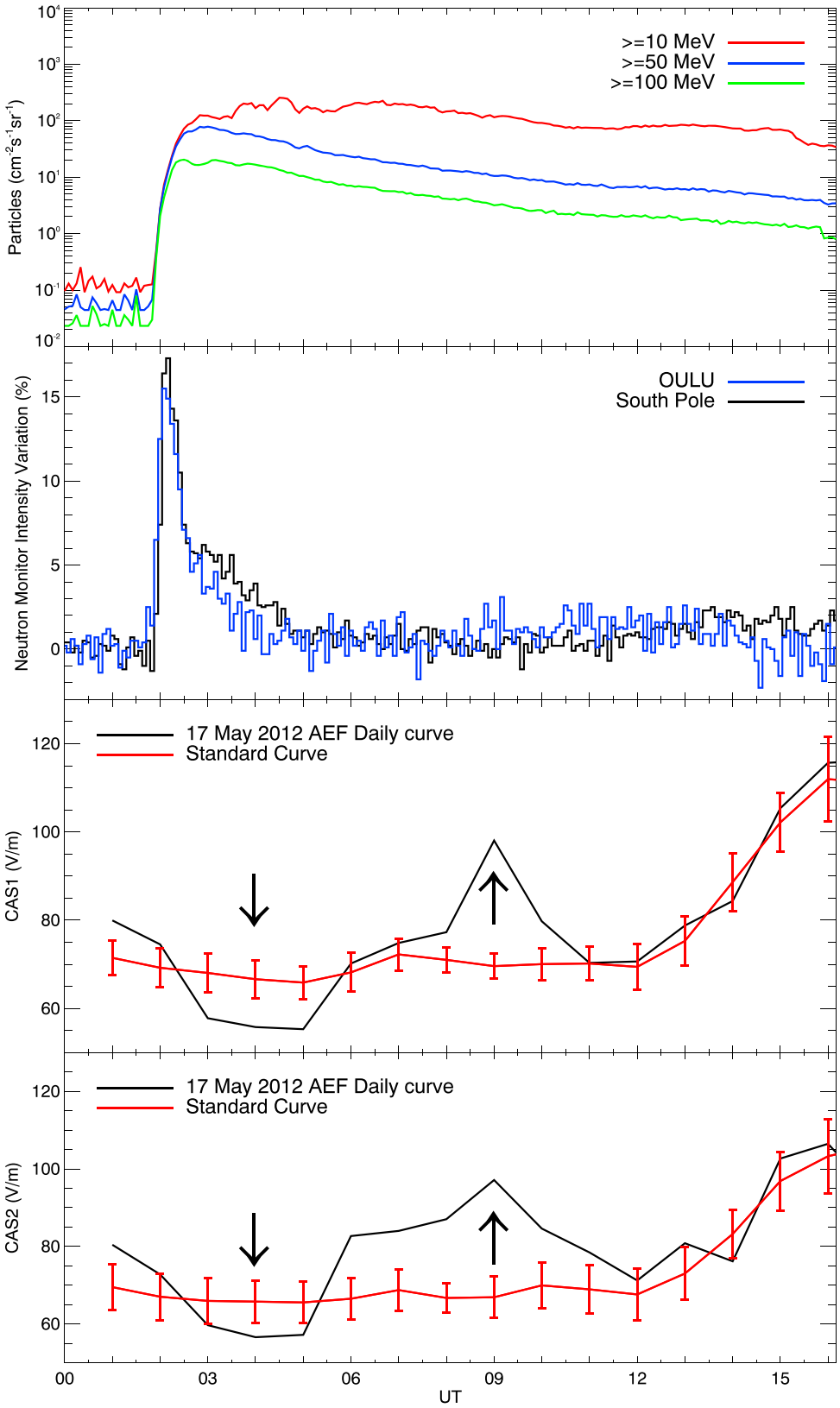

Figure 3. (first panel) Energetic protons flux in the channels ≥10 MeV (red curve), ≥50 MeV (blue curve), and ≥100 MeV (green curve). (second panel) Neutron monitor count rate enhancements at South Pole (black curve) and Oulu (blue curve) stations. (third panel) CAS1 AEF hourly values for the day of the event (black curve) and the monthly standard curve (red curve) with their respective error bars of one standard deviation (1σ). (fourth panel) Same as third panel but for CAS2 station data.

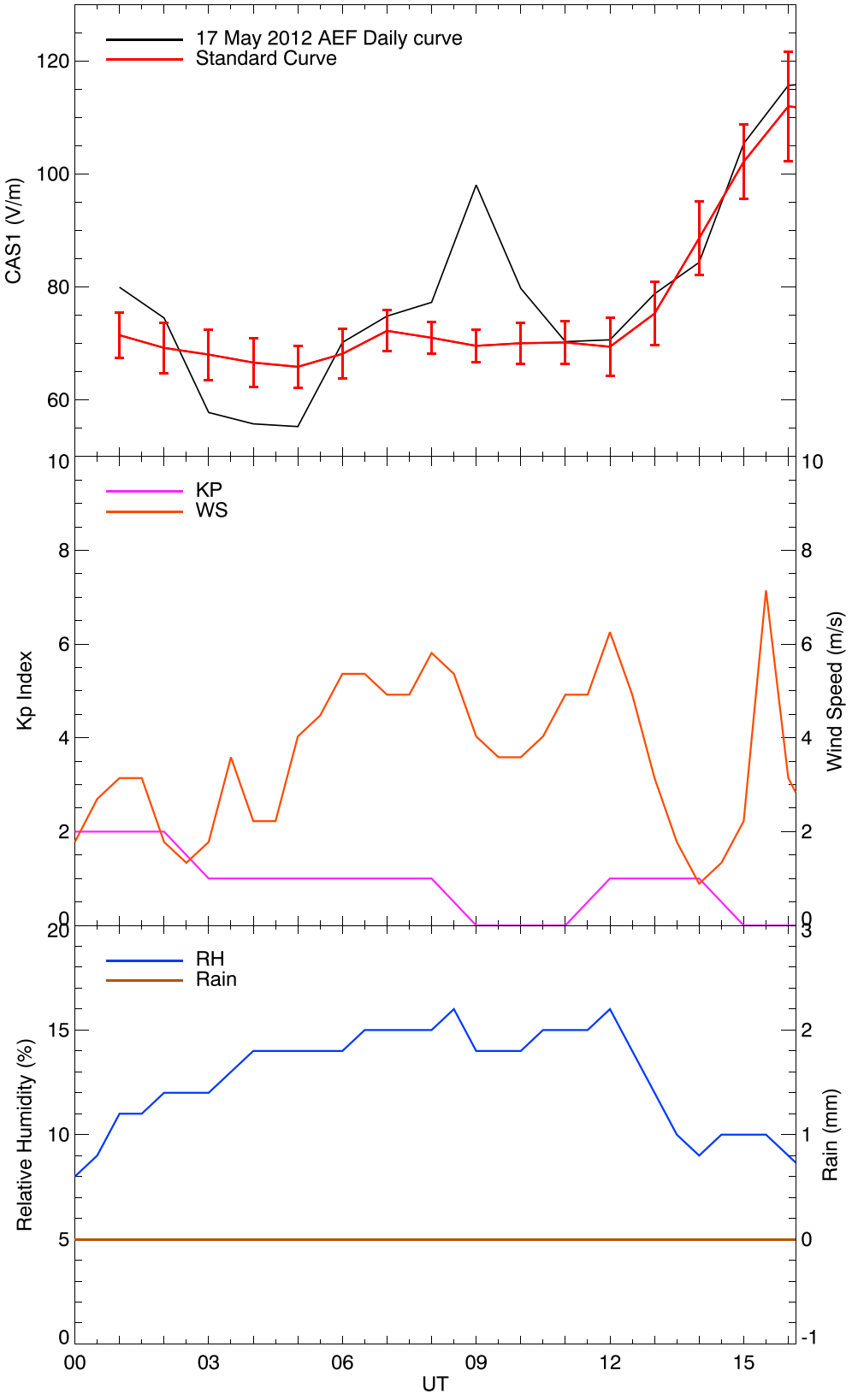

Figure 4. The evolution of the atmospheric electric field, geomagnetic, and meteorological activity on 17 May 2012. (top) The same as the third panel of Figure 3. (middle) The *Kp* index (purple line) and wind speed (WS, orange line). (bottom) The relative humidity (RH, blue line) and rain (brown line).

deviation values can be observed after the start of the solar proton event (hour zero). This increase corresponds to an excess ~13% over mean values.

During the period of analysis, one of the 15 solar proton events that occurred on 17 May 2012 catches our attention (details of the 15 SPEs are summarized in Appendix A). This solar proton event was strong enough to produce a ground level enhancement (GLE), named GLE71 (https://gle.oulu.fi/#/). Further analysis was done to determinate whether the GLE effect was crucial to obtain the result presented in Figure 2. For that, we remove completely this event from the analysis keeping only 14 solar proton events to which the superposed epoch analysis was applied (blue dashed curve). The result was very similar, with insignificant discrepancies.

We have analyzed in more details the event of 17 May 2012 (GLE71). Figure 3 shows at the first panel the GOES proton flux for three energy channels: ≥100 MeV (green curve), ≥50 MeV (blue curve), and ≥10 MeV (red curve). The second panel shows the cosmic ray ground level enhancement (GLE) observed by two neutron monitors: South Pole (black curve) and Oulu (blue curve). The third and fourth panels display the AEF monthly standard curve for May 2012 (red curve) and the atmospheric electric field measurements recorded on the day of the GLE event at CAS1 and CAS2 (black curves). In this figure, the error bars represent one standard deviation (1σ) of the mean.

Figure 3 shows evidence that, during the proton flux increases, and until its maximum, high energetic particles produced an enhancement in the neutron monitor measurements. Just after the start of the cosmic ray enhancement, the atmospheric electric field variation starts to deviate toward negative values. Then, a significant decrease of the atmospheric electric field is observed to last for ~3 hr. This first response is indicated by an arrow pointing down. Later, ~7 hr after the start of the solar proton event, the atmospheric electric field response is positive and presents higher values with respect to its mean values. This positive excess is illustrated by an arrow pointing up, maximizes at ~09 UT, before recovering standard curve values after ~11:30 UT.

To discard any geomagnetic storm and/or meteorological effect in the behavior of the atmospheric electric field during the GLE71, the global geomagnetic activity and local atmospheric conditions were examined during the time period 00–16 UT. Figure 4 shows (i) the atmospheric electric field deviation relative to the monthly standard curve recorded at CAS1 (the same as the third panel of Figure 3) in the top panel, (ii) the planetary *Kp* index used to characterize any geomagnetic activity and the wind speed in the middle panel, and (iii) the relative humidity and the rain precipitation in the bottom panel.

Figure 4 shows that the geomagnetic and atmospheric conditions were quiet during the development of the GLE. Despite the wind speed presents short-term variations, it remained always below 8 m/s, which is characteristic of fair weather conditions with no meteorological influence on the atmospheric electric field measurements (Harrison, 2013). The period of interest is also characterized by zero level of rain precipitation. Relative humidity measurements indicate clear- and dry sky conditions, with recorded values below 15%, that is, well below the levels that can produce variations in the AEF measurements (Bennett & Harrison, 2007). Therefore, the results presented in Figure 4 strongly suggest that the significant excesses observed in the atmospheric electric field may be related to the solar proton event/GLE that occurred on 17 May 2012.

5. Discussions and Conclusions

In this paper, we show results on the atmospheric electric field (AEF) variations under fair weather (FW) conditions, measured at ground level, during solar flares without solar proton events (SPEs), case I, and during intense SPEs, case II. In order to do that, we discard events for which Forbush decreases and/or geomagnetic storms are observed in the time period [−1 day, +2 days] around the event start time.

For case I (see Figure 1), no significant changes of the atmospheric electric field values were found. It means that there are no considerable AEF deviations (excess) of the "curve I" compared with the "background curve." This is not a surprise since the enhanced low-energy X-ray and UV radiations are absorbed above ~60 km of altitude (Mironova et al., 2015). This is well above the region where variations of conductivity are likely to affect the flow of current in the global atmospheric electric circuit (GAEC).

Therefore, any direct effect of solar flare photons on the GAEC seems unlikely to produce changes on the AEF measured in fair weather regions.

On the other hand, case II shows a significant effect on the atmospheric electric field values (see Figure 2). We note an increase about ~10 V/m from fair weather standard values, which corresponds to an excess of ~13%. This increase only occurs between ~3 and 8 hr after the start of the solar proton event. Our results are in agreement with previous works. Cobb (1967) found a maximum deviation of 10% from mean values on the air-Earth current one day after solar flares at Mauna Loa (3,400 m asl). In the same way, Reiter (1969, 1971) found a maximum increase about 60% and 25% on the atmospheric electric field values at 2,964 and 1,780 m asl one day after solar flares, respectively. This increase lasted until three to four days after the solar event but with less intensity. It is worth to mention that in these works, solar proton event and solar flares events (not followed by any SEP event) are not treated separately. Besides that, and differently from what has been done in the present study, they do not consider the possible effect of other solar, interplanetary, and geomagnetic phenomena (as coronal mass ejections, geomagnetic storm, and Forbush decreases).

Considering exclusively solar flare and solar proton event influences on the atmospheric electric field, our results show that only SPEs can produce an increase on the atmospheric electric field in fair weather regions with duration of some hours after the start of the event. This result is supported qualitatively by models proposed by several authors (Farrell & Desch, 2002; Markson, 1978; Willett, 1979). Markson (1978) postulated that energetic charged particles increase the ionization rate above the thunderstorm generator changing the resistance and therefore the atmospheric conductivity in this region. Since disturbed weather regions include most of the global atmospheric electric circuit ohmic resistance, the region above thunderstorms behaves like a valve regulating the upward flowing current. The resistance above fair weather regions, in this part of the global electric circuit, is affected but there is little or no change because this resistance is weak. Then, an increase of the electrical potential is expected in the upper boundary of the GAEC above fair weather regions, which will result in a similar increase of the atmospheric electric field. In the same way, Farrell and Desch (2002) also proposed that the atmospheric conductivity profile increase above thunderstorm increasing the upward current and therefore producing an increase on the atmospheric electric field in fair weather regions on the ground level. Regardless of the different existing models, we must emphasize that all of them result in an increase on the AEF in FW regions on the ground level after intense solar proton events. Thus, our results agree with these previous works performed at other locations.

A still open question is quantitatively how much the increase of the atmospheric electric field after solar proton events should be? The model proposed by Markson (1978) proposed an increase of about 40% while Willet (1979) found a maximum increase ~16%. The difference between both models is principally due to the nature of the thundercloud as source: while Markson (1978) assumes the thundercloud as a voltage source, Willett (1979) assumes it as a current source. More discussions on these two possibilities can be found in Slyunyaev et al. (2015). Farrell and Desch (2002) proposed that the excess of the atmospheric electric field depends on the number of thunderstorms affected by the solar proton events. Their predictions show excesses from 10% to 20% for 1,000 and 2,000 thunderstorms affected by the SPE, respectively. The increase found by models, Willett (1979) and Farrell and Desch (2002), and observations, Cobb (1967), agree with our result expecting an increase on the order of 10%.

Besides the increase related to solar energetic particles influence on the global atmospheric electric circuit discussed above, we also observed a decrease event probably related to a local effect. Figure 3 shows a significant decrease of the atmospheric electric field values in the event where the solar proton event was accompanied by a ground level enhancement (GLE) that occurred on 17 May 2012. This decrease which shows the same duration as the GLE could be related to a direct increase in the ground ionization at the measurement site during a fair weather period. GLEs are very intense events that produce secondary high-energy particles reaching the ground level. Secondary neutrons generated in this process were observed by South Pole and Oulu neutron monitor (second panel of Figure 3). We note a maximum increase at ~2 UT, which lasted until ~6 UT for South Pole. During the same period, we observe a decrease of the atmospheric electric field values for CAS1 and CAS2 electric field mill stations. We suggest that this effect can be related to a local ground ionization increase produced by an

increase of the secondary high-energy particle flux. We propose that these particles ionize the Earth's surface causing an increase in the atmospheric conductivity. By Ohm's law and taking into account that the air-Earth current density is constant, we expect a decrease of the atmospheric electric field as observed in Figure 3. This similar decreasing behavior of the atmospheric electric field has been observed by balloon measurements during solar proton events (Holzworth et al., 1987; Holzworth & Mozer, 1979; Kokorowski et al., 2006; Reagan et al., 1983). Therefore, it is possible that the same process affects the ground level conductivity when a very intense solar proton event is accompanied by a GLE. Figure 3 also shows an increase (~6 hr later after the start of the GLE). As discussed previously, we believe that this increase is produced by the excess of the atmospheric ionization produced above thunderstorms (i.e., in disturbed weather regions). Then, for this particular event, we observe a local effect, which is immediate, and a global effect, which takes time to produce perturbations on the global electric circuit (which is evidenced in Figure 2, where the increase of the AEF is approximately 3–8 hr after the start of the solar proton event).

It is worth to note that, in the superposed epoch analysis plot (Figure 2), we do not observe a significant decrease on the atmospheric electric field values after the solar proton event beginning when analyzing all events together. This can be due to the fact that the solar proton event of 17 May 2012 was the only that was accompanied by a GLE event during the studied period. The solar proton events included on the superposed epoch technique were intense but not strong enough to cause changes in the ionization on the ground level.

In summary, we investigate the effect of solar events on the global atmospheric electric circuit through the analysis of the atmospheric electric field variations in fair weather regions. No significant effect was found during solar flares without solar proton occurrence, suggesting that solar flare photons are unlikely to modify the global electric circuit. However, our results suggest that intense solar proton events may modify the conductivity in areas above thunderstorms (disturbed weather regions) affecting the global electric circuit in fair weather regions. Furthermore, we observe that very intense solar proton event (occurred together with a ground level enhancement) can produce changes on the ionization which modifies the atmospheric conductivity and, therefore, altering the atmospheric electric field on the Earth's surface in fair weather regions.

Appendix A: Solar Proton Event List

Table A1 lists the 15 solar proton events chosen according to the criteria described in section 3. Information was obtained from ftp://ftp.swpc.noaa.gov/pub/indices/SPE.txt, ftp://ftp.swpc.noaa.gov/pub/warehouse, and https://cdaw.gsfc.nasa.gov/CME_list/. The only one classified as GLE during 2010–2015 was 17 May 2012 (GLE71; https://gle.oulu.fi/#/).

Table A1
List of the 15 Solar Proton Events Chosen for Our Analysis

	Solar Proton Event (≥100 MeV)		Associated CME		
Year	Start Date/Time (UT)	Proton Fluence (protons/cm^2 day sr)	First C2 Appearance Date/Time (UT)	Central PA (deg)	Linear Speed (km/s)
2011	21 March/04:00	8.4e + 03	21 March/02:24	Halo	1341
2011	23 September/02:00	7.7e + 03	23 September/00:48	105	1116
2012	27 January/18:00	1.6e + 05	27 January/18:27	Halo	2508
2012	17 May/02:00	3.2e + 05	17 May/01:48	Halo	1582
2012	12 July/17:00	3.7e + 03	12 July/16:48	Halo	885
2012	19 July/07:00	1.9e + 04	19 July/05:24	Halo	1631
2012	23 July/07:00	2.9e + 04	23 July/02:36	Halo	2003
2012	28 September/01:00	5.0e + 03	28 September/00:12	Halo	947
2013	11 April/08:00	7.0e + 04	11 April/07:24	Halo	861
2013	15 May/12:00	2.8e + 03	15 May/01:48	Halo	360
2013	22 May/14:00	9.4e + 04	22 May/13:25	Halo	1466
2013	30 September/02:00	6.5e + 03	29 September/22:12	Halo	1179
2014	06 January/08:00	9.4e + 04	06 January/08:00	Halo	1402
2014	07 January/19:00	6.1e + 04	07 January/18:24	Halo	1830
2014	18 April/13:00	1.3e + 04	18 April/13:25	Halo	1203

Acknowledgments

J.T. would like to thank CAPES (finance code 001) for the funding. J.P.R. and J.T. would like to thank CNPq for the funding (project 422253/2016-2). R.R.S. M. thanks the China-Brazil Joint Laboratory for Space Weather. Data availability is described at the following websites: https://theafinsa.wordpress.com/data-download/ (atmospheric electric field), https://gle.oulu.fi/#/ (neutron monitor), and https://umbra.nascom.nasa.gov/sdb/goes/ (solar flares and solar proton events). The authors thank the reviewers for their constructive comments and suggestions, which helped to improve the quality of the paper.

References

APRE (IT), & DST (ZA) (2013). Report on global research infrastructures: A first mapping exercise, EURORISONET, accessed on: May 9, 2018. Retrieved from http://www.euroris-net.eu/sites/www.euroris-net.eu/files/EuroRIs-Ne%2B_Global_RI_Report_2013.pdf

Bazilevskaya, G. A. (2005). Solar cosmic rays in the near Earth space and the atmosphere. *Advances in Space Research*, *35*(3), 458–464. https://doi.org/10.1016/j.asr.2004.11.019

Bennett, A. J., & Harrison, R. G. (2007). Atmospheric electricity in different weather conditions. *Weather*, *62*(10), 277–283. https://doi.org/10.1002/wea.97

Chubb, J. (2014). The measurement of atmospheric electric fields using pole mounted electrostatic fieldmeters. *Journal of Electrostatics*, *72*(4), 295–300. https://doi.org/10.1016/j.elstat.2014.05.002

Cobb, W. E. (1967). Evidence of a solar influence on the atmospheric electric elements at Mauna Loa observatory. *Monthly Weather Review*, *95*(12), 905–911. https://doi.org/10.1175/1520-0493(1967)095<0905:EOASIO>2.3.CO;2

Elhalel, G., Yair, Y., Nicoll, K., Price, C., Reuveni, Y., & Harrison, R. G. (2014). Influence of short-term solar disturbances on the fair weather conduction current. *Journal of Space Weather and Space Climate*, *4*, A26. https://doi.org/10.1051/swsc/2014022

Farrell, W. M., & Desch, M. D. (2002). Solar proton events and the fair weather field at ground. *Geophysical Research Letters*, *29*(9), 1323. https://doi.org/10.1029/2001GL013908

Haldoupis, C., Rycroft, M., Williams, E., & Price, C. (2017). Is the "Earth-ionosphere capacitor" a valid component in the atmospheric electric circuit? *Journal of Atmospheric and Solar-Terrestrial Physics*, *164*, 127–131. https://doi.org/10.1016/j.jastp.2017.08.012

Harrison, R. G. (2013). The Carnegie curve. *Surveys in Geophysics*, *34*(2), 209–232. https://doi.org/10.1007/s10712-012-9210-2

Holzworth, R., & Mozer, F. S. (1979). Direct evidence of solar flare modification of stratospheric electric field. *Journal of Geophysical Research*, *84*(A6), 2559–2566. https://doi.org/10.1029/JA084iA06p02559

Holzworth, R. H., Norville, K. W., & Williamson, P. R. (1987). Solar flares perturbations in stratospheric current systems. *Geophysical Research Letters*, *14*(8), 852–855. https://doi.org/10.1029/GL014i008p00852

Kokorowski, M., Sample, J. G., Holzworth, R. H., Bering, E. A., Bale, S. D., Blake, J. B., et al. (2006). Rapid fluctuations of stratospheric electric field following a solar energetic particle event. *Geophysical Research Letters*, *33*, L20105. https://doi.org/10.1029/2006GL027718

Kokorowski, M., Seppälä, A., Sample, J. G., Holzworth, R. H., McCarthy, M. P., Bering, E. A., & Turunen, E. (2012). Atmosphere-ionosphere conductivity enhancements during a hard solar energetic particle event. *Journal of Geophysical Research*, *117*, A05319. https://doi.org/10.1029/2011JA017363

Liu, C., Williams, E., Zipser, E. J., & Burns, G. (2010). Diurnal variations of global thunderstorms and electrified shower clouds and their contribution to the global electrical circuit. *Journal of the Atmospheric Sciences*, *67*(2), 309–323. https://doi.org/10.1175/2009JAS3248.1

Mach, D. A., Blakeslee, J., & Bateman, M. (2011). Global electric circuit implications of combined aircraft storm electric current measurements and satellite-based diurnal lightning statistics. *Journal of Geophysical Research*, *116*, D05201. https://doi.org/10.1029/2010JD014462

Markson, R. (1978). Solar modulation of atmospheric electrification and possible implications for the Sun-weather relationship. *Nature*, *273*(5658), 103–109. https://doi.org/10.1038/273103a0

Mironova, I. A., Aplin, K. L., Arnold, F., Bazilevskaya, G. A., Harrison, R. G., Krivolutsky, A. A., et al. (2015). Energetic particle influence on the Earth's atmosphere. *Space Science Reviews*, *194*(1-4), 1–96. https://doi.org/10.1007/s11214-015-0185-4

Nicoll, K. A., & Harrison, R. G. (2014). Detection of lower tropospheric responses to solar energetic particles at midlatitudes. *Physical Review Letters*, *112*(22), 225,001 (1-5). https://doi.org/10.1103/PhysRevLett.112.225001

Reagan, J. B., Meyerott, R. E., Evans, J. E., Imhof, W. L., & Joiner, R. G. (1983). The effects of energetic particle precipitation on the atmospheric electric circuit. *Journal of Geophysical Research*, *88*(C6), 3869–3878. https://doi.org/10.1029/JC088iC06p03869

Reiter, R. (1969). Solar flares and their impact on potential gradient and air-Earth current characteristic at high mountain stations. *Pure and Applied Geophysical*, *72*(1), 259–267. https://doi.org/10.1007/BF00875709

Reiter, R. (1971). Further evidence for impact of solar flares on potential gradient and air-Earth current characteristics at high mountain stations. *Pure and Applied Geophysical*, *86*(1), 142–158. https://doi.org/10.1007/BF00875081

Rycroft, M. J., Harrison, R. G., Nicoll, K. A., & Mareev, E. A. (2008). An overview of Earth's global electric circuit and atmospheric conductivity. *Space Science Reviews*, *137*(1–4), 83–105. https://doi.org/10.1007/s11214-008-9368-6

Rycroft, M. J., Nicoll, K. A., Aplin, K. L., & Harrison, R. G. (2012). Recent advances in global electric circuit between the space environment and the troposphere. *Journal of Atmospheric and Solar-Terrestrial Physics*, *90-91*, 198–211. https://doi.org/10.1016/j.jastp.2012.03.015

Sapkota, B. K., & Varshneya, N. C. (1990). On the global atmospheric electrical circuit. *Journal of Atmospheric and Terrestrial Physics*, *52*(1), 1–20. https://doi.org/10.1016/0021-9169(90)90110-9

Sartor, D. (1980). Electric field perturbations in terrestrial clouds and solar flare events. *Monthly Weather Review*, *198*, 499–505.

Secker, P. E. (1975). The design of simple instrumentation for measurement of charge on insulating surfaces. *Journal of Electrostatics*, *1*(1), 27–36. https://doi.org/10.1016/0304-3886(75)90005-4

Sheftel, V. M., Bandilet, O. I., Yaroshenko, A. N., & Chernyshev, A. K. (1994). Space-time structure and reasons of global, regional, and local variations of atmospheric electricity. *Journal of Geophysical Research*, *99*(D5), 10,797–10,806. https://doi.org/10.1029/93JD02857

Slyunyaev, N. N., Mareev, E. A., & Zhidkov, A. A. (2015). On the variation of the ionospheric potential due to large-scale radioactivity enhancement and solar activity. *Journal of Geophysical Research: Space Physics*, *120*, 7060–7082. https://doi.org/10.1002/2015JA021039

Tacza, J., Raulin, J.-P., Macotela, E., Norabuena, E., Fernandez, G., Correia, E., et al. (2014). A new south American network to study the atmospheric electric field and its variations related to geophysical phenomena. *Journal of Atmospheric and Solar-Terrestrial Physics*, *120*, 70–79. https://doi.org/10.1016/j.jastp.2014.09.001

Takagi, Y., & Iwata, A. (1984). *Solar influence on the Earth's electric field, paper presented at seventh international conference on atmospheric electricity*. Albany, NY: American Meteorological Society. Jun 4-8

Velinov, P. I. Y., Asenovski, S., Kudela, K., Lastovicka, J., Mateev, L., Mishev, A., & Tonev, P. (2013). Impact of cosmic rays and solar energetic particles on the Earth's ionosphere and atmosphere. *Journal of Space Weather and Space Climate*, *3*, A14. https://doi.org/10.1051/swsc/2013036

Whipple, F. J. W. (1929). On the association of the diurnal variation of electric potential gradient in fine weather with the distribution of thunderstorms over the globe. *Quarterly Journal of the Royal Meteorological Society*, *55*, 1–17.

Willett, J. C. (1979). Solar modulation of the supply current for atmospheric electricity? *Journal of Geophysical Research*, *84*(C8), 4999–5002. https://doi.org/10.1029/JC084iC08p04999

Wilson, C. T. R. (1921). Investigations on lightning discharges and on the electric field of thunderstorms. *Philosophical Transactions of the Royal Society of London*, *221A*, 73–115.